Numerical Algorithms
https://doi.org/10.1007/s11075-019-00751-5

ORIGINAL PAPER

High-precision computation of the weak Galerkin methods for the fourth-order problem

John Burkardt[1] · **Max Gunzburger**[2] · **Wenju Zhao**[2,3]

Received: 20 February 2019 / Accepted: 4 June 2019 / Published online: 25 June 2019

Abstract
The weak Galerkin form of the finite element method, requiring only C^0 basis function, is applied to the biharmonic equation. The computational procedure is thoroughly considered. Local orthogonal bases on triangulations are constructed using various sets of interpolation points with the Gram-Schmidt or Levenberg-Marquardt methods. Comparison and high-precision computations are carried out, and convergence rates are provided up to degree 11 for L^2, 10 for H^1, and 9 for H^2, suggesting that the algorithm is useful for a variety of computations.

Keywords Weak Galerkin · Fourth-order problem · Orthogonal basis · High precision

Mathematics Subject Classification (2010) 65N30 · 35J30

1 Introduction

The power of the finite element method (FEM) comes in part from the idea of a weak solution. Instead of requiring that a solution satisfies the partial differential equation

✉ Wenju Zhao
wz13@my.fsu.edu

John Burkardt
burkardt@vt.edu

Max Gunzburger
mgunzburger@fsu.edu

[1] Department of Mathematics, Virginia Polytechnic Institute and State University, Blacksburg, VA 24061, USA

[2] Department of Scientific Computing, Florida State University, Tallahassee, FL 32304, USA

[3] Department of Mathematics, Southern University of Science and Technology, Shenzhen, 518055 Guangdong, China

(PDE) at every point in the domain (termed a "strong" solution), FEM transforms the PDE into an integral variational formulation which projects the equation onto a finite dimensional space of test functions. This approach, combined with the use of integration by parts, allows FEM to recover "weak solutions" to problems which classical methods cannot handle. The success of FEM has inspired extensions to handle even more general classes of domains, boundary conditions, operators, discontinuities, and stochastic behavior, including nonconforming elements, isoparametric elements, discontinuous Galerkin FEM, and collocation approaches. In particular, there is a recent addition to the FEM family, called the weak Galerkin method [11, 17–23], etc., which is the focus of this paper.

Over the years, FEM has been primarily applied to PDEs of second order, where a great deal of theory, technique, and software is available. However, the situation is not nearly so satisfactory in the case of fourth-order PDEs, of which the biharmonic equation $\Delta^2 u = f$ is the classic example. Difficulties arise because of the higher degree of differentiation, and because the boundary conditions must be treated with greater care. When classical FEM methods are applied to the biharmonic equation, elements of class C^1 are commonly employed for conforming approximation of the weak solution of the PDE. Typical elements include the well-oriented Bogner-Fox-Schmit element and its extension on quadrilateral elements [24], and the Argyris [6] and Bell elements [5], both of which are associated with a triangulated mesh. In general, however, it is difficult to construct and manipulate the corresponding C^1 finite element space.

In contrast, the weak Galerkin (WG) finite element method offers highly flexible element construction, using discontinuous piecewise polynomials on a general partition, including polygons of arbitrary shape [19]. It can get any desired order of accuracy by selecting the appropriate local polynomial basis functions. WG also admits the use of totally discontinuous functions in the finite element procedure. In general, WG greatly simplifies the task of constructing the C^1 finite element space. The primary task in implementing WG is then the construction of the weak gradient operator in cases involving a second-order PDE [18, 22], or the weak Laplacian operator symbolized by Δ_w, for fourth-order problems [17, 19]. Numerical implementation of the second-order problem has been studied [18]. In this paper, we will focus on the fourth-order problems, typified by the biharmonic equation, to see how to obtain high-precision simulations. The main contributions of this paper:

- Studying of the fourth-order elliptic equation is a counterpart of computation study of weak Galerkin method for second-order elliptic equation [18].
- This paper generalizes the WG-Algorithm in [19, 20] to a range of eligible local basis pairings (see Algorithm 1) and the optimal local basis pairings are numerically found (see Section 6.2).
- The construction and comparison of the local orthogonal bases and Lagrange bases on Gaussian points (see Section 4) are tested which are merely mentioned in existing papers for weak Galerkin methods. Discretized systems with the local orthogonal bases are much more efficiently solvable.

– The relatively high convergence tests, i.e., degree 11 for L^2, 10 for H^1, and 9 for H^2, are numerically considered as a benefit of easy programming among the existing numerical methods for biharmonic equation.

The remainder of this paper is organized as follows: in Section 2, we present the model biharmonic problem, and compare traditional and WG approaches to its solution; Section 3 discusses the formulation of WG-FEM and its local discretizations; in Section 4, miscellaneous techniques associated with discrete WG-FEM are presented; Section 6 presents numerical experiments; Section 7 contains conclusions.

2 The model problem

Let Ω be some two-dimensional domain, with a Lipschitz continuous boundary denoted by $\partial\Omega$, and $\hat{n}$ the unit outward normal vector to $\partial\Omega$. Consider the following biharmonic system,

$$\Delta^2 u = f \text{ in } \Omega, \tag{2.1}$$

$$u = g \text{ on } \partial\Omega, \tag{2.2}$$

$$\nabla u \cdot \hat{n} = h \text{ on } \partial\Omega, \tag{2.3}$$

where we require $u \in H^2(\Omega)$, $f \in L^2(\Omega)$, and $g, h \in L^2(\partial\Omega)$. Finite element approaches to solve the model problem (2.1)–(2.3) begin by constructing a space of trial functions with specific smoothness, considering the inner product of the model equation with generic test functions, and applying integration by parts to arrive at a variational form of the problem. Within this general structure, there are a number of different approaches possible. To see how WG differs from the usual FEM approaches, and where its advantages lie, we outline several common finite element methods applied to the model problem.

2.1 $H^2(\Omega)$ conforming FEM

For the H^2 conforming finite element approach, the corresponding variational formulation of (2.1)–(2.3) is posed by seeking $u \in H^2(\Omega)$ satisfying $u|_{\partial\Omega} = g$ and $\frac{\partial u}{\partial \hat{n}}|_{\partial\Omega} = h$ such that

$$(\Delta u, \Delta v) = (f, v), \ \forall v \in H_0^2(\Omega), \tag{2.4}$$

where $(\cdot, \cdot)$ is the L^2 inner product on Ω, and $H_0^2(\Omega)$ is the subspace of $H^2(\Omega)$ with vanishing traces of functions and normal derivatives on $\partial\Omega$ (cf.[1]).

2.2 $H^1(\Omega)$-mixed FEM

The mixed finite element method can be applied to the fourth-order problem with some specific boundary conditions. By introducing intermediate variables $w = u$, $v = -\Delta u$ and setting the boundary condition (2.2)–(2.3) to be homogeneous, we can write the biharmonic (2.1)–(2.3) as a system of coupled second-order equations.

After constructing test function spaces for w and v, we arrive at a variational formulation (see [14]) which seeks $(u, v) \in H_0^1 \times H^1(\Omega)$ such that

$$\begin{aligned}(\nabla w, \nabla \phi) &= (v, \phi), \ \forall \phi \in H^1(\Omega),\\ (\nabla v, \nabla \psi) &= (f, \psi), \forall \psi \in H_0^1(\Omega),\end{aligned} \tag{2.5}$$

where $H^1(\Omega)$ is the space of functions with L^2 derivatives in Ω, and $H_0^1(\Omega)$ is the subset of $H^1(\Omega)$ with zero trace (cf.[1]).

2.3 $H^1(\Omega)$ discontinuous Galerkin FEM

For the discontinuous Galerkin method, we must introduce a triangulation $\mathcal{T}_h$ (or some other spatial discretization) of Ω. Let $\mathcal{E}_I$ and $\mathcal{E}_B$ be the set of interior edges and boundary edges of $\mathcal{T}_h$, respectively, and let $\mathcal{E}_h = \mathcal{E}_I \cup \mathcal{E}_B$. Let $T_i, T_j \in \mathcal{T}_h$ and assume T_i and T_j share the common interface $e \in \mathcal{E}_I$. The jump across e and the mean value of $u \in H^1(\Omega, \mathcal{T}_h)$, as described in [16], are defined by $[u]_e = u|_{\partial T_i \cap e} - u|_{\partial T_j \cap e}$ and $\{u\}_e = \frac{1}{2}(u|_{\partial T_i \cap e} + u|_{\partial T_j \cap e})$. For each $e \in \mathcal{E}_I$, we associate the unit normal vector n directed from T_i to T_j, and for each $e \in \mathcal{E}_B$, $\hat{n}$ is the outward unit normal vector. See [16], we introduce the bilinear form

$$B(u, v) = B_\Delta(u, v) + B_s(u, v),$$

with

$$\begin{aligned}B_\Delta(u, v) &= \sum_{T \in \mathcal{T}_h} (\Delta u, \Delta v)_{L^2(T)} + \sum_{e \in \mathcal{E}_h} \Big(< \{\frac{\partial \Delta u}{\partial n}\}, [v] >_e + < [u], \{\frac{\partial \Delta v}{\partial n}\} >_e \\ &\quad - < \{\Delta u\}, [\frac{\partial v}{\partial n}] >_e - < [\frac{\partial u}{\partial n}], \{\Delta v\} >_e \Big),\\ B_s(u, v) &= \sum_{e \in \mathcal{E}_h} \Big(< \alpha_T [u], [v] >_e + < \beta_T [\frac{\partial u}{\partial n}], [\frac{\partial u}{\partial n}] >_e \Big),\end{aligned}$$

and the linear functional $l(v) = l_\Delta(v) + l_s(v)$ with

$$\begin{aligned}l_\Delta(v) &= (f, v)_{L^2(\Omega)} - < g, \frac{\partial \Delta v}{\partial \hat{n}} >_{L^2(\partial\Omega)} + < h, \Delta v >_{L^2(\partial\Omega)},\\ l_s(v) &= \sum_{e \in \mathcal{E}_B} < \alpha_T g, v >_e + < \beta_T h, \frac{\partial v}{\partial \hat{n}} >_e,\end{aligned}$$

where $< \cdot, \cdot >$ denotes the L^2 boundary inner product, and the constants $\alpha_T \geq 0$ and $\beta_T \geq 0$ depend on the discretization parameters. Then, a general discontinuous weak formulation of the biharmonic equation (2.2)–(2.3) reads: find $u \in H^4(\Omega, \mathcal{T}_h)$ such that

$$B(u, v) = l(v), \ \forall v \in H^4(\Omega, \mathcal{T}_h), \tag{2.6}$$

where the space $H^4(\Omega, \mathcal{T}_h)$ is defined in [16].

2.4 Weak Galerkin FEM

Weak Galerkin finite element methods [17, 19, 20] inherit some properties from the discontinuous version of FEM, including stability, and the treatment of discontinuities. Like the discontinuous Galerkin method, the weak Galerkin method depends heavily on the spatial discretization $\mathcal{T}_h$. In particular, the weak Galerkin method forms the function space incrementally, by constructing an appropriate function space associated with each constituent element of the spatial discretization, and then combining them. Given element $T \in \mathcal{T}_h$, define the local weak function space as a triple

$$V(T) = \{v = \{v_0, v_b, \mathbf{v}_g\} : v_0 \in L^2(T), v_b \in H^{1/2}(\partial T), \mathbf{v}_g \cdot n \in H^{-1/2}(\partial T)\}.$$

By patching together the spaces $V(T)$ over all the elements $T \in \mathcal{T}_h$, and requiring common values on the interface $\mathcal{E}_I \in \mathcal{T}_h$, we arrive at the global weak function space

$$V(\Omega) = \{\{v_0, v_b, \mathbf{v}_g\} : \{v_0, v_b, \mathbf{v}_g\}|_T \in V(T), \forall T \in \mathcal{T}_h\}.$$

Let V^0 be the subspace of V with vanishing trace on $e \in \mathcal{E}_B$,

$$V^0(\Omega) = \{\{v_0, v_b, \mathbf{v}_g\} \in V(\Omega) : v_b|_e = 0, \mathbf{v}_g \cdot \hat{n}|_e = 0, e \in \mathcal{E}_B\}.$$

For the definition of the weak Laplacian space, we define a local space $G(T)$,

$$G(T) = \{v_w : v_w \in H^1(T), \Delta v_w \in L^2(T)\},$$

and the element-wise space

$$G(\Omega) = \{v_w : v_w|_T \in G(T), T \in \mathcal{T}_h\}.$$

We introduce the local weak Laplacian Δ_w of $v = \{v_0, v_b, \mathbf{v}_g\} \in V(T)$ as a linear functional in the dual space of $G(T)$, for $\forall v_w \in G(T)$

$$(\Delta_w v, v_w)_T = (v_0, \Delta v_w)_T - < v_b, \nabla v_w \cdot n >_{\partial T} + < \mathbf{v}_g \cdot n, v_w >_{\partial T}, \quad (2.7)$$

where n is the outward unit normal vector to ∂T and $< \cdot, \cdot >_{\partial T}$ is the inner product on $L^2(\partial T)$. Then, the global weak Laplacian can be obtained by patching the local operators together:

$$(\Delta_w u, \Delta_w w) := \sum_{T \in \mathcal{T}_h} (\Delta_w u, \Delta_w w)_T. \quad (2.8)$$

Finally, the weak Galerkin finite element method can be presented as: seek $u = \{u_0, u_b, \mathbf{u}_g\} \in V(\Omega)$ such that for $v = \{v_0, v_b, \mathbf{v}_g\} \in V^0(\Omega)$,

$$(\Delta_w u, \Delta_w v) + s(u, v) = (f, v_0), \tag{2.9}$$

where the stabilizer term $s(u, v)$ is used to enforce the connectivity between pairs of discrete subdomains and to regularize the discrete system. This term is similar to the case in the DG-FEM (2.6), where we have:

$$s(u_h, v) := \sum_{T \in \mathcal{T}_h} \alpha_T < u_0 - u_b, v_0 - v_b >_{\partial T} \tag{2.10}$$

$$+ \sum_{T \in \mathcal{T}_h} \beta_T < \nabla u_0 - \mathbf{u}_g, \nabla v_0 - \mathbf{v}_g >_{\partial T} . \tag{2.11}$$

Remark 1 WG-FEM retains the advantages of the DG-FEM (2.6) and reduces the difficulty of constructing basis functions in $H^2(\Omega)$ as in (2.4), and makes it much easier to apply Neumann boundary conditions compared with (2.4) and (2.5). Although the notation used is somehow complex, the actual implementation is simpler.

3 Formulation and discretization of WG-FEM

WG-FEM uses a weak finite element space of totally discontinuous functions, allowing great flexibility in the construction of the local basis. With a further consideration of $\mathbf{u}_g$ in (2.10). we have a quantity of interest of the directional gradient, $\mathbf{u}_g \cdot \hat{n} = \nabla u \cdot \hat{n}$. Letting $\mathbf{u}_g = (u_1, u_2)$, $\hat{n} = (n_1, n_2)$, it follows an underdetermined equation

$$u_1 \hat{n}_1 + u_2 \hat{n}_2 = \nabla u \cdot \hat{n}, \tag{3.1}$$

which gives us some choices to construct the basis $\mathbf{u}_g$. Given a unit vector $\tilde{n}$ with $\tilde{n} \cdot \hat{n} \neq 0$, we define $\mathbf{u}_g = u_g \tilde{n}$ which implies

$$u_g \tilde{n} \cdot \hat{n} = \nabla u \cdot \hat{n} \Rightarrow u_g = \frac{\nabla u \cdot \hat{n}}{\tilde{n} \cdot \hat{n}}.$$

A straightforward choice is to select $\tilde{n}$ parallel to $\hat{n}$ and with $\tilde{n} \cdot \tilde{n} = 1$. Let us introduce a set of normal directions on $\mathcal{E}_h$ as

$$D_h = \{\mathbf{n}_e : \mathbf{n}_e \text{ is an unit normal vector to } e, e \in \mathcal{E}_h\}.$$

To further reduce the unknowns of the discrete system, using normal component approximation, the sub-stabilizer term in (2.10) with $\mathbf{u}_g = u_g\mathbf{n}_e$, $\mathbf{v}_g = v_g\mathbf{n}_e$, $\mathbf{n}_e \in D_h$, $T \in \mathcal{T}_h$ (see [19]) is induced to

$$\begin{aligned} < \nabla u_0 - \mathbf{u}_g, \nabla v_0 - \mathbf{v}_g >_{\partial T} &= < \nabla u_0 - u_g\mathbf{n}_e, \nabla v_0 - v_g\mathbf{n}_e >_{\partial T} \\ &\simeq < \nabla u_0 \cdot \mathbf{n}_e - u_g, \nabla v_0 \cdot \mathbf{n}_e - v_g >_{\partial T} . \end{aligned}$$

Algorithm 1 WG-FEM for the Biharmonic equation.

Let a weak discrete Galerkin finite element space $V_h(\Omega) \subset V(\Omega)$ be

$$\begin{aligned} V_h(\Omega) &= \{v = \{v_0, v_b, v_g\mathbf{n}_e\} : v|_T \in V_h(T), T \in \mathcal{T}_h\}, \\ V_h(T) &= \{v_0 \in P_l(T), v_b \in P_m(e), v_g \in P_n(e), e \subset \partial T\}, \end{aligned}$$

and a weak Laplacian space be

$$\begin{aligned} G_h(\Omega) &= \{v_w : v_w|_T \in G_h(T), T \in \mathcal{T}_h\}, \\ G_h(T) &= \{v_w \in P_w(T), \Delta v_w \in L^2(T)\}, \end{aligned}$$

with $\max(l-2, 0) \le m, n, w \le l+2, l, m, n, w \in \mathbb{N}^+$. Then a numerical approximation for (2.1)–(2.3) can be obtained by seeking $u_h = \{u_0, u_b, u_g\mathbf{n}_e\} \in V_h$ satisfying for all $v_h = \{v_0, v_b, u_g\mathbf{n}_e\} \in V_h^0$

$$(\Delta_w u_h, \Delta_w v_h) + s(u_h, v_h) = (f, v_0), \tag{3.2}$$

with the stabilizer term

$$\begin{aligned} s(u_h, v) := &\sum_{T\in\mathcal{T}_h} \alpha_T < u_0 - u_b, v_0 - v_b >_{\partial T} \\ &+ \sum_{T\in\mathcal{T}_h} \beta_T < \nabla u_0 \cdot \mathbf{n}_e - u_g, \nabla v_0 \cdot \mathbf{n}_e - v_g >_{\partial T}, \end{aligned}$$

where $\mathbf{n}_e \subset D_h$ and $\alpha_T = O(h_T^{-3})$ and $\beta_T = O(h_T^{-1})$, i.e., $\alpha_T = (\max|e|)^{-3}$ and $\beta_T = (\max|e|)^{-1}$, $e \in \partial T$ (cf. [16,17]).

3.1 The local discretization of WG-FEM

It should be clear that WG-FEM is understood by concentrating on the local representations; the properties of the full discrete system then follow from the combination of the weakly coupled local information.

3.1.1 The local discrete basis function

In considering WG-FEM, it is important to make a clear distinction between the effective domain of the local weak basis functions and the support of their local weak Laplacian. Since these concepts are easily confused, it is worth presenting an explanation from the computational point of view. Let $T \in \mathcal{T}_h$ with interior T_0 and boundary ∂T, so that $T_0 \cup \partial T = T$; further, let $K_0, K_b, K_g, K_w \in \mathbb{N}^+$ representing the degree of polynomials, while N_0, N_b, N_g, N_w are the dimensions of the corresponding polynomial spaces; let $v_0^l, l = 1, \ldots, N_0$ be a set of interior

basis functions for $P_{K_0}(T_0)$, and $v_b^l, l = 1, \ldots N_b$ a set of boundary basis functions for $\sum_{e\in\partial T\cap\mathcal{E}_h} P_{K_b}(e)$ and $v_g^l, l = 1, \ldots N_g$ a set of boundary basis functions for $\sum_{e\in\partial T\cap\mathcal{E}_h} P_{K_g}(e)$. Then, every local discrete weak function $v = \{v_0, v_b, v_g\mathbf{n}_e\} \in V_h(T)$ can be written into a three-part sum as follows

$$v|_T = \{v_0, v_b, v_g\mathbf{n}_e\}|_T = \sum_{l=1}^{N_0} c_0^l\{v_0^l, 0, 0\} + \sum_{l=1}^{N_b} c_b^l\{0, v_b^l, 0\} + \sum_{l=1}^{N_g} c_g^l\{0, 0, v_g^l\mathbf{n}_e\},$$

which, for convenience, we may abbreviate as

$$v|_T = \{v_0, v_b, v_g\mathbf{n}_e\}|_T = \sum_{l=1}^{N_0} c_0^l v_0^l + \sum_{l=1}^{N_b} c_b^l v_b^l + \sum_{l=1}^{N_g} c_g^l v_g^l\mathbf{n}_e.$$

Here $\{c_0^l\}, \{c_b^l\}, \{v_g^l\}$ are the corresponding coefficients and we have used the notations $v_0^l := \{v_0^l, 0, 0\}$, $v_b^l := \{0, v_b^l, 0\}$, $v_g^l := \{0, 0, v_g^l\mathbf{n}_e\}$.

We now refer to properties of the Lagrange interpolation polynomial basis function. The local interior basis functions $\{v_0^l\}$ are represented in Fig. 1a; the local boundary basis functions $\{v_b^l\}$ and $\{v_g^l\}$ in Fig. 1b and c, respectively. The local degrees of freedom (DOF) for the weak Galerkin method are *the number of interior basis* $\{v_0\}$ + *the number of edge basis* $\{v_b\}$ + *the number of edge basis* $\{v_g\}$. For instance, in Fig. 1, $P_{K_0}(T) = P_7(T)$, $P_{K_b}(e) = P_7(e)$, $P_{K_g}(e) = P_6(e)$, and hence the local DOF counts $36 + 3 \times 8 + 3 \times 7 = 81$. The total global DOF counts *the element number* $\times$ *the number of local interior basis* (v_0) + *the edge number* $\times$ *the number of local boundary basis* (v_b) + *the edge number* $\times$ *the number of local boundary basis* (v_g).

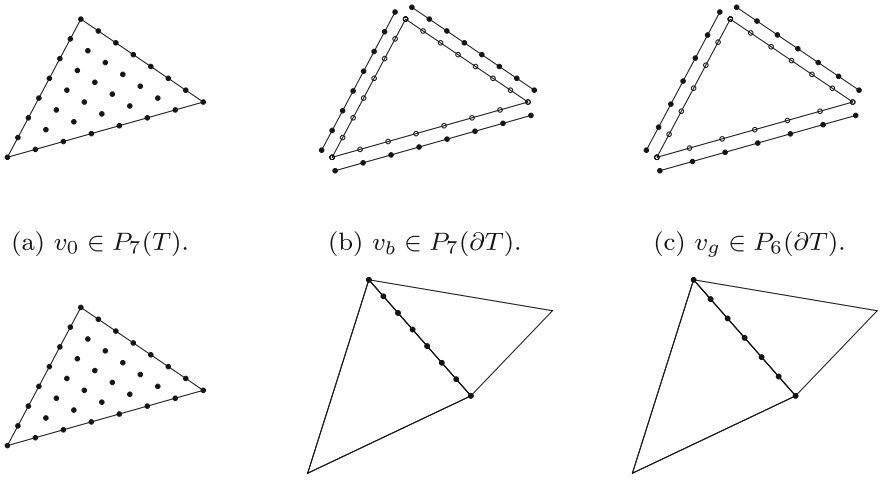

(a) $v_0 \in P_7(T)$. (b) $v_b \in P_7(\partial T)$. (c) $v_g \in P_6(\partial T)$.

(d) Support of $\Delta_w v_0$. (e) Support of $\Delta_w v_b$. (f) Support of $\Delta_w v_g$.

Fig. 1 Locations of local basis functions and corresponding supports

Let us further explain what the weak function $v = \{v_0, v_b, \mathbf{n}_g\} \in V(T)$ means in the region T. The functions v_0 and v_b can be considered as representing the value of v in the interior and on the boundary of T; then, $\mathbf{n}_g$ represents the derivative information for v on the boundary ∂T. However, the interior basis v_0 need not share the same trace as the basis function v_b on the edge; further, they are completely independent. Also note that the boundary basis functions on different edges that share a vertex are completely different; they represent different information on different edges. The global weak function over an entire domain is constructed as a combination of discontinuous local functions defined over all the individual elements. The element edges play crucial roles in communicating information between adjacent elements. For weak Laplacian of a weak function defined in T_0 or on ∂T, the support of the interior basis function v_0 is just one element, as indicated in Fig. 1d, whereas the support of the boundary basis functions v_b and v_g is generally a pair of adjacent elements, as shown in Fig. 1e and f, respectively.

There is a closed relationship between classical H^2 functions and weak functions. A local weak function $v \in V(T)$ is said to be in $H^2(T)$ if it can be identified with a function $\tilde{v} \in H^2(T)$ through the inclusion map i_W [19]

$$i_W(\tilde{v})|_T = \{\tilde{v}|_T, \tilde{v}|_{\partial T}, \nabla\tilde{v}|_T, \Delta\tilde{v}|_T\}.$$

It is not hard to check that the weak Laplacian $\Delta_w v$ is identical to the strong Laplacian Δv in $H^2(T)$. The Sobolev space $H^2(T)$ can be embedded into the space $V(T)$ by an inclusion map i_W.

3.1.2 The local discrete weak Laplacian

For the conforming finite element approximation (2.4), the Lapacian operator Δ is meant to represent the classical weak second derivative of an $H^2(\Omega)$ function. The definition of the weak Laplacian operator Δ_w in (2.7) makes WG-FEM different from methods (2.4), (2.5), (2.6). For the weak Galerkin finite element method, the polynomial spaces used to approximate the weak basis functions v and their weak Laplacian $\Delta_w v$ may be the same, or different, providing an extra degree of flexibility. Numerical experiments in Section 6 show that the precision of computational results can be increased by increasing the degree of a discrete weak Laplacian space $G_h(\Omega)$ with a fixed discrete weak function $V_h(\Omega)$.

Based on the definition of the weak Laplacian (2.7), we have that, for a given local discrete weak function $v \in V_h(T)$, the discrete weak Laplacian $(\Delta_w)_h v \in P_{K_w}(T) \subset G(T)$ is defined as for all $v_w \in P_{K_w}(T)$

$$((\Delta_w)_h v, v_w)_T = (v_0, \Delta v_w)_T - < v_b, \nabla v_w \cdot n >_{\partial T} + < v_g \mathbf{n}_e \cdot n, v_w >_{\partial T} . \quad (3.3)$$

Let $v_w^l, l = 1, \ldots, N_w$ be a set of basis functions of $P_{K_w}(T) \subset G(T)$. For convenience, in the subsequent the same notation $\Delta_w := (\Delta_w)_h$ will be used to represent the discrete weak Laplacian operator. The discrete weak Laplacian $\Delta_w v \in P_{K_w}(T)$ has a representation

$$\Delta_w v|_T = \sum_{l=1}^{N_w} c_w^l v_w^l, \ \ v_w^l \in P_{K_w}(T). \quad (3.4)$$

Further, local discrete weak Laplacians of all the basis functions $\{v_0^l\}$, $\{v_b^l\}$, $\{v_g^l\}$ can be written in matrix form

$$\begin{bmatrix} \Delta_w v_0^{\mathbf{l}} \\ \Delta_w v_b^{\mathbf{l}} \\ \Delta_w v_g^{\mathbf{l}} \end{bmatrix} = \begin{bmatrix} C_0 \\ C_b \\ C_g \end{bmatrix}_{N_{0,b,g} \times N_w} [v_w^{\mathbf{l}}]_{N_w \times 1}, \tag{3.5}$$

where $N_{0,b,g} = N_0 + N_b + N_g$, and $\Delta_w v_0^{\mathbf{l}} = [\Delta_w v_0^1, \ldots, \Delta_w v_0^{N_0}]^T$, $\Delta_w v_b^{\mathbf{l}} = [\Delta_w v_b^1, \ldots, \Delta_w v_b^{N_b}]^T$, $\Delta_w v_g^{\mathbf{l}} = [\Delta_w v_g^1, \ldots, \Delta_w v_g^{N_g}]^T$, $[v_w^{\mathbf{l}}]_{N_w \times 1} = [v_w^1, \ldots, v_w^{N_w}]^T$ are column vectors, and C_0, C_b, C_g matrices of coefficients whose values need to be determined. The local matrices may be produced by taking the inner product with each local basis function $v_w^l \in P_{K_w}(T), l = 1, ..., N_w$ on the left part of (3.3):

$$M_{v_w} = \begin{bmatrix} (v_w^1, v_w^1)_T & \ldots & (v_w^{N_w}, v_w^1)_T \\ \vdots & \ddots & \vdots \\ (v_w^1, v_w^{N_w})_T & \ldots & (v_w^{N_w}, v_w^{N_w})_T \end{bmatrix}.$$

On the right-hand side of (3.3), for each term, we have the following corresponding matrix forms, respectively,

$$M_{v_0} = \begin{bmatrix} (v_0^1, \Delta v_w^1)_T & \ldots & (v_0^{N_0}, \Delta v_w^1)_T \\ \vdots & \ddots & \vdots \\ (v_0^1, \Delta v_w^{N_w})_T & \ldots & (v_0^{N_0}, \Delta v_w^{N_w})_T \end{bmatrix},$$

$$M_{v_b} = \begin{bmatrix} < v_b^1, \nabla v_w^1 \cdot n >_{\partial T} & \ldots & < v_b^{N_b}, \nabla v_w^1 \cdot n >_{\partial T} \\ \vdots & \ddots & \vdots \\ < v_b^1, \nabla v_w^{N_w} \cdot n >_{\partial T} & \ldots & < v_b^{N_b}, \nabla v_w^{N_w} \cdot n >_{\partial T} \end{bmatrix},$$

$$M_{v_g} = \begin{bmatrix} < v_g^1 \mathbf{n}_e \cdot n, v_w^1 >_{\partial T} & \ldots & < v_g^{N_g} \mathbf{n}_e \cdot n, v_w^1 >_{\partial T} \\ \vdots & \ddots & \vdots \\ < v_g^1 \mathbf{n}_e \cdot n, v_w^{N_w} >_{\partial T} & \ldots & < v_g^{N_g} \mathbf{n}_e \cdot n, v_w^{N_w} >_{\partial T} \end{bmatrix},$$

where the Laplace operator Δ and the gradient operator ∇ are the classical instances rather than the weak Laplacian Δ_w and ∇_w in [22]. Combining them, we have the following system:

$$M_{v_w} C_{0,b,g} = [M_{v_0}, -M_{v_b}, M_{v_g}] \tag{3.6}$$

with $C_{0,b,g} = [C_0^T, C_b^T, C_g^T]$. Once the matrices $M_{v_w}, M_{v_0}, M_{v_b}, M_{v_g}$ are computed, we can obtain the coefficient matrix $C_{0,b,g}$. Transposing and multiplying $C_{0,b,g}$ by $[v_w^{\mathbf{l}}]_{N_w \times 1}$ produces the representations of the discrete weak Laplacians of all the basis function $\{v_0\}, \{v_b\}, \{v_g\}$. This indicates significant difference between WG-FEM and H^2-conforming finite element method (2.4). Here, the weak Laplacian $\Delta_w v$ is approximated by the dual space of P_{K_w} instead of the real Laplacian information.

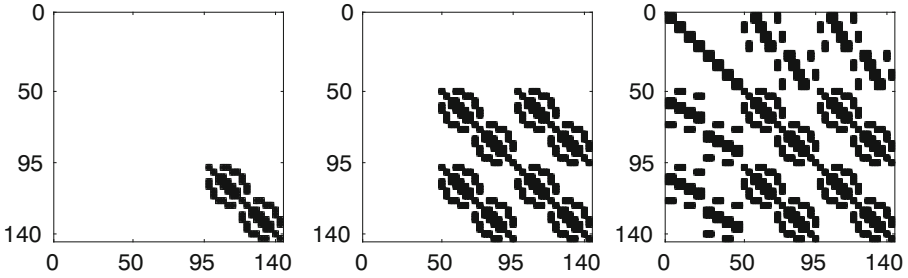

Fig. 2 Contributions of discrete weak Laplacian terms to global sparse matrix

Before introducing the stabilizer term, let us look further into the contribution of the weak Laplacian to the global matrix system. The lower degrees of the weak Laplacian spaces $P_{K_w}(T)$, $K_w \leq 1$ are interesting spaces for large scale simulations. When $K_w = 0$, the definition of the discrete weak Laplacian (3.3) can be simplified to:

$$(\Delta_w v, v_w)_T = < v_g \mathbf{n}_e \cdot n, v_w >_{\partial T}, v_w \in P_{K_w=0}(T). \tag{3.7}$$

and when $K_w = 1$, the expression (3.3) reduces to for all $v_w \in P_{K_w=1}(T)$

$$(\Delta_w v, v_w)_T = - < v_g, \nabla v_w \cdot n >_{\partial T} + < v_g \mathbf{n}_e \cdot n, v_w >_{\partial T} . \tag{3.8}$$

For both cases, it is easily shown that the weak Laplacian of any interior basis function $\{v_0\}$ is exactly zero, so that there will be no contribution to the global matrix system. As examples, in Figs. 2, 3, and 4, the sparse matrix structures are generated

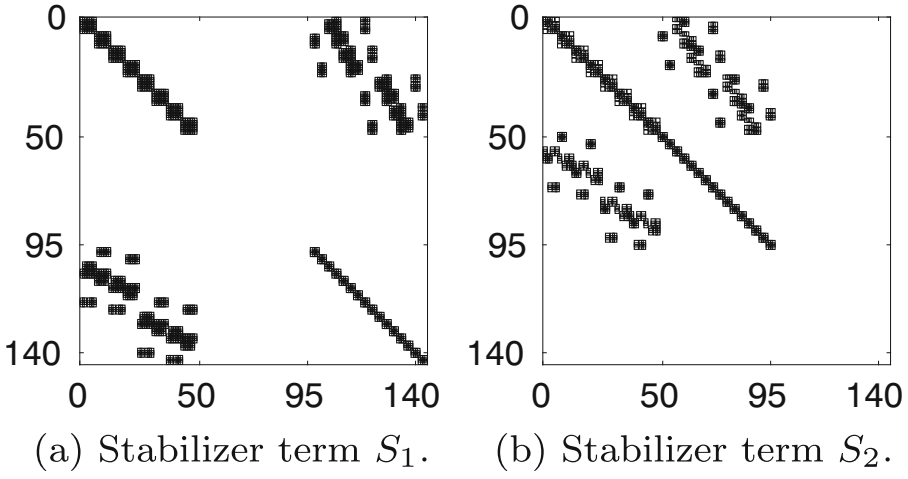

Fig. 3 Contributions of discrete stabilizer terms to global sparse matrix

with a specific discrete weak Galerkin function space,

$$V_h(\Omega) = \{v = \{v_0, v_b, v_g \mathbf{n}_e\} : v|_T \in V_h(T), T \in \mathcal{T}_h\},$$
$$V_h(T) = \{v_0 \in P_2(T), v_b \in P_2(e), v_g \in P_2(e), e \subset \partial T\}$$

and discrete weak Laplacian spaces $G_h(T) = \{P_0(T), P_1(T), P_2(T)\}, T \in \mathcal{T}_h$, respectively, defined on an uniform triangulation of $[0, 1]^2$ with 8 elements.

3.1.3 The Local discrete stabilizer term

Figure 2 illustrates the fact that, for the lower order polynomial spaces $P_{K_w}(T) \subset G(T)$, $K_w \leq 1$, the discrete system

$$(\Delta_w u_h, \Delta_w v_h) = (f, v_0), \tag{3.9}$$

will be of indefinite type. This implies that stabilizer terms will be indispensable. In other nonconforming finite element methods, such as isoparametric-FEM or DG-FEM, a common idea to regularize the system (3.9) is to add terms associated with the edges and boundaries of the partitioned domain, which increases the connectivity of adjacent elements. As in Algorithm 1, the local stabilizer term is written as

$$\begin{aligned} s(u_h, v)|_{\partial T} : &= \alpha_T < u_0 - u_b, v_0 - v_b >_{\partial T} + \beta_T \\ &< \nabla u_0 \cdot \mathbf{n}_e - u_g, \nabla v_0 \cdot \mathbf{n}_e - v_g >_{\partial T} = S_1 + S_2 \end{aligned} \tag{3.10}$$

with

$$S_1 = \alpha_T < u_0, v_0 >_{\partial T} + \alpha_T < u_b, v_b >_{\partial T},$$
$$S_2 = \beta_T < \nabla u_0 \cdot \mathbf{n}_e, \nabla v_0 \cdot \mathbf{n}_e >_{\partial T} + \beta_T < u_g, v_g >_{\partial T} .$$

Now let

$$u|_T = \{u_0, u_b, u_g \mathbf{n}_e\}|_T = \sum_{l=1}^{N_0} c_0^l \{u_0^l, 0, 0\} + \sum_{l=1}^{N_b} c_b^l \{0, u_b^l, 0\} + \sum_{l=1}^{N_g} c_g^l \{0, 0, u_g^l \mathbf{n}_e\},$$

and substitute this form into (3.10), and take the boundary inner product from $\{u_0^l\}$ to $\{u_b^l\}$, then to $\{u_g^l\}$. Then, we have a local matrix of the discrete stabilizer term as

$$\begin{bmatrix} \alpha_T M_{01} + \beta_T M_{02} & & \\ & \alpha_T M_b & \\ & & \beta_T M_c \end{bmatrix}$$

with

$$M_{01} = \begin{bmatrix} < u_0^1, u_0^1 >_{\partial T} & \cdots & < u_0^{N_0}, u_0^1 >_{\partial T} \\ \vdots & \ddots & \vdots \\ < u_0^1, u_0^{N_0} >_{\partial T} & \cdots & < u_0^{N_0}, u_0^{N_0} >_{\partial T} \end{bmatrix},$$

$$M_{02} = \begin{bmatrix} < \nabla u_0^1 \cdot \mathbf{n}_e, \nabla u_0^1 \cdot \mathbf{n}_e >_{\partial T} & \cdots & < \nabla u_0^{N_0} \cdot \mathbf{n}_e, \nabla u_0^1 \cdot \mathbf{n}_e >_{\partial T} \\ \vdots & \ddots & \vdots \\ < \nabla u_0^1 \cdot \mathbf{n}_e, \nabla v_0^{N_b} \cdot \mathbf{n}_e >_{\partial T} & \cdots & < \nabla u_0^{N_0} \cdot \mathbf{n}_e, \nabla u_0^{N_0} \cdot \mathbf{n}_e >_{\partial T} \end{bmatrix},$$

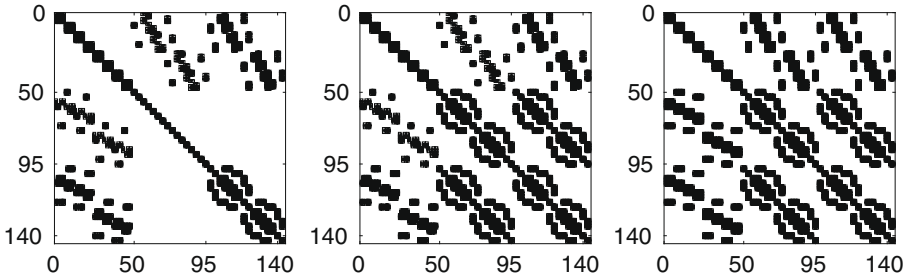

(a) $G_h(T) = P_0$. (b) $G_h(T) = P_1$. (c) $G_h(T) = P_2$.

Fig. 4 Sparsity patterns for different weak Laplacian spaces

$$M_b = \begin{bmatrix} < u_b^1, u_b^1 >_{\partial T} & \cdots & < u_b^{N_b}, u_b^1 >_{\partial T} \\ \vdots & \ddots & \vdots \\ < u_b^1, u_b^{N_b} >_{\partial T} & & < u_b^{N_b}, u_b^{N_b} >_{\partial T} \end{bmatrix},$$

$$M_c = \begin{bmatrix} < u_g^1, u_g^1 >_{\partial T} & \cdots & < u_g^{N_g}, u_g^1 >_{\partial T} \\ \vdots & \ddots & \vdots \\ < u_g^1, u_g^{N_b} >_{\partial T} & \cdots & < u_g^{N_g}, u_g^{N_b} >_{\partial T} \end{bmatrix}.$$

Figure 3 illustrates how the stabilizer terms contribute to the global sparse matrix.

Figure 4 shows the structures of global matrix systems with different weak Laplacian spaces as in Section 3.1.2. Higher sparsity can be achieved by using orthogonal basis functions, so that most of the small block matrices are reduced to diagonal forms. While the WG-FEM method may generate more degrees of freedom than comparable methods, that drawback is outweighted by a high sparsity of the resulting system matrices.

4 Construction of reference basis

A significant advantage of the WG-FEM derives from the fact that the piecewise discontinuous function spaces are used for both in the interior domain $T_0 \in \mathcal{T}_h$ and on the edge $e \in \mathcal{E}_h$. This provides flexibility in the construction of the local reference basis functions. Often, a hierarchical basis function space is chosen. For non-hierarchical basis function spaces, the Lagrange interpolation polynomials are the most useful tools. As we have seen, with an orthogonal basis here offers a high sparsity of a global matrix system. In this section, we will focus on how to construct a variety of basis function spaces on a reference triangle domain (simplex). Other polygonal domains, such as rectangles or hexagons, can easily be patched together from triangular subdomains. In the following, we focus on the two-dimensional space domain. The cases of 3D and higher can be similarly constructed.

4.1 The hierarchical basis

The hierarchical basis function space is interesting not only for its own sake, but it can be used as a tool to construct several other basis function spaces. For a 2D simplex, the spaces can be described as $P_n = \text{span}\{x^l y^k : l, k \geq 0, l + k \leq n\}$. An orthogonal basis can be constructed from a hierarchical basis with Gram-Schmidt procedure (see Example 1).

4.2 The Lagrange interpolation basis for simplices

The Lagrange approach is a method of choice for dealing with polynomial interpolation. Several other polynomial spaces can be induced by starting from an uniformly spaced Lagrange interpolation space, which depend primarily on the choice of the number and position of the interpolation points. Theoretically, Lagrange interpolation using uniformly spaced points has a beautiful mathematical formula [4], in which all the coefficients are rational numbers. However, when equally spaced interpolation points are chosen, the Runge phenomenon arises, so that small perturbations in the data may lead to huge changes in the interpolant. The associated interpolation matrix will be very ill-conditioned [3] for high-degree equidistant interpolation functions.

4.2.1 Equidistant interpolation points

Assume the reference domain is an unit triangle with vertices $(0, 0)$, $(1, 0)$, $(0, 1)$. The barycentric coordinate system provides an useful method of indexing points within the reference triangle. If the value d represents the degree of the desired polynomial space, we assign indices i and j to the nodes in the obvious way, then add an auxiliary index $k = d - i - j$. A node whose barycentric indices are (i, j, k) has the barycentric coordinates $(\frac{i}{d}, \frac{j}{d}, \frac{k}{d})$. Now, as is typical in Lagrange interpolation, each Lagrange basis function will be associated with a particular node. The formula of a polynomial basis function associated with a barycentric index (i, j, k) is (see [4])

$$\phi(i, j, k)(x, y) = \prod_{l=0}^{i-1}(x - \frac{l}{d}) \prod_{l=0}^{j-1}(y - \frac{l}{d}) \prod_{l=0}^{k-1}((1 - x - y) - \frac{l}{d}).$$

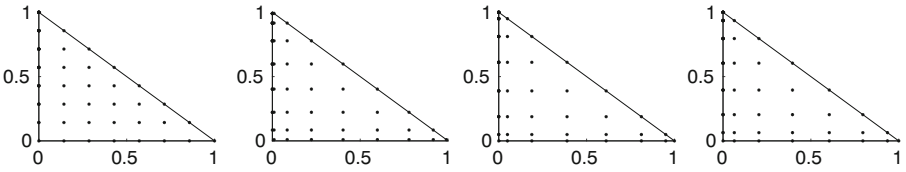

(a) Equidistant. (b) Chebyshev 1. (c) Chebyshev 2. (d) Gauss Lobatto.

Fig. 5 Lagrange nodal sets for P_{10}^2

4.2.2 Miscellaneous interpolation points

Because of the Runge's phenomenon, Lagrange interpolation is more often carried out using Chebyshev points or other Gauss points (Fig. 5). Chebyshev points have a geometric structure obtained by projecting equally spaced points on an unit semicircle down to an unit interval $[-1, 1]$. The Chebyshev points of the first kind (Chebyshev 1) are given as

$$x_l = \cos \frac{(2l+1)\pi}{2N+2}, \quad l = 0, \ldots, N,$$

and the second kind (Chebyshev 2) are given as

$$x_l = \cos \frac{l\pi}{N}, \quad l = 0, 1, \ldots, N.$$

Interpolation polynomials on a simplex have been investigated on a variety of interpolation points, including Gauss-Lobatto and Chebyshev-Gauss (see [12]). If a set of interpolation points $\{x_l\}$ is proposed, the corresponding Lagrange interpolating polynomials $\{\psi_l : \psi_l(x_k) = \delta_{l,k}\}$ can be constructed with uniformly spaced basis function $\{\phi_l\}$ as

$$\psi_l = \sum_{k=0}^{N} c_{l,k}\phi_k, \quad l = 0, 1, \ldots, N.$$

The enforcement at all interpolation points $\{x_l\}$ results in a linear system as

$$\begin{bmatrix} \phi_1(x_0) & \ldots & \phi_N(x_0) \\ \vdots & \ddots & \vdots \\ \phi_1(x_N) & \ldots & \phi_N(x_N) \end{bmatrix} \begin{bmatrix} c_{0,1} & \ldots & c_{N,1} \\ \vdots & \ddots & \vdots \\ c_{0,N} & \ldots & c_{N,N} \end{bmatrix} = \begin{bmatrix} 1 & \ldots & 0 \\ \vdots & \ddots & \vdots \\ 0 & \cdots & 1 \end{bmatrix}.$$

4.3 The orthogonal basis

Figures 2, 3, and 4 show that, with Lagrange basis, the global matrix system will typically exhibit a pattern of small block matrices. Many of these block matrices can actually be replaced by diagonal matrices if an interpolation basis is replaced by an orthogonal basis.

4.3.1 1D orthogonal basis

Although there are several ways to construct 1D orthogonal basis functions, the most popular method is used a three-term recurrence formula

$$a_{l+1}\psi_{l+1}(x) = (x - b_n)\psi_l(x) - a_l\psi_{l-1}(x), \; l = 1, 2, ... \tag{4.1}$$

Now let $\{\psi_l\}_1^\infty$ be a set of orthonormal polynomials with respect to a weight function $w(x)$ on the unit line L such that

$$\int_L \psi_l(x)\psi_k(x)w(x)dx = \delta_{l,k}, \; l, k \in \mathbb{N}^+.$$

The orthogonal polynomials $\{\psi_l\}$ satisfy a specific kind of three-term recurrence relation (4.1), The connection between the nonnegative integrable function $w(x)$ and the real sequences $\{a_l\}_{l=1}^{\infty}$, $\{b_l\}_{l=1}^{\infty}$ has been widely studied. Different pairs lead to a variety of orthogonal bases. Readers can refer to [8, 10] for details.

4.3.2 2D-triangle orthogonal basis

Ridar [9] has studied orthogonal systems in the Bernstein-Bézier form on triangular domains. With the help of the symbolic computation facilities of Maple or Mathematica, and nonlinear solvers, a given polynomial basis can be transformed into an orthogonal basis, which may further be chosen to have hierarchical form if desired.

Now let P be a polynomial space on a triangle T with an inner product $(\cdot,\cdot)_T$, and suppose that $\{\phi_l\}_{l=1}^{N}$ is a known basis for P. A set of functions $\{\psi_l\}_{l=1}^{N}$ is said to be orthogonal over the element T if

$$(\psi_l, \psi_k)_T = \int_T \psi_l \psi_k dx = \delta_{l,k},\ l, k = 1, 2, \ldots, N.$$

A straightforward procedure is combined Gram-Schmidt orthogonalization and symbolic computation with Maple or Mathematica. The Gram-Schmidt orthogonalization procedure has the form

$$\begin{aligned}
\psi_1 &= \phi_1/(\phi_1, \phi_1)_T, \\
\psi_2 &= \phi_2 - (\phi_2, \psi_1)_T \psi_1, \\
&\cdots \\
\psi_N &= \phi_N - (\phi_N, \psi_1)_T \psi_1 - \cdots - (\phi_N, \psi_{N-1})_T \psi_{N-1}.
\end{aligned}$$

After normalization, the set $\{\psi_l\}_{l=1}^{N}$ will be an orthonormal basis on the triangle T. In a standard way, information on a reference triangle T can be transformed to any arbitrary triangle with affine transformation.

An orthogonal basis can be also found numerically using a nonlinear solver. Suppose that, for an element T, $\{\phi_l\}$ is a known set of basis functions, while $\{\psi_l\}$ is a (presumably unknown) set of orthonormal basis functions. Then, by the basis property, there exist coefficients $c_{l,k}$, so that:

$$\psi_l = \sum_{k=1}^{N} c_{l,k} \phi_k, \quad l = 1, 2, \ldots, N.$$

Now the basis functions $\{\psi_l\}$ satisfy an orthogonality condition

$$(\psi_l, \psi_k)_T = \delta_{l,k} \text{ (Kronecker delta)},$$

which further can be rewritten in terms of the basis functions $\{\phi_l\}$,

$$\sum_{k,l=1}^{N} c_{i,l} c_{j,k} (\phi_l, \phi_k)_T = \delta_{i,j},\ i, j = 1, \ldots, N. \tag{4.2}$$

Table 1 Basis functions of $P_1(T)$

Hierarchical basis	Orthogonal basis	Lagrange basis	Orthogonal basis
1	2	$1-y-x$	$12-12y-12x$
x	$12x-8$	x	$\frac{84}{31}x+\frac{72}{31}y-\frac{72}{31}$
y	$\frac{40x}{37}+\frac{4y}{37}-\frac{88}{111}$	y	$\frac{2223072}{981151}x+\frac{2569404}{981151}y-\frac{2211912}{981151}$

The induced nonlinear system (4.2) generally has many solutions, but a least squares Levenberg-Marquardt nonlinear method [15] can be used to effectively find a solution, allowing us to recombine the known basis $\{\phi_l\}$ so as to construct a realization of an orthonormal basis $\{\psi_l\}$.

Example 1 Basis functions of P_1 in hierarchical and Lagrange forms complied with corresponding orthogonal basis functions are listed in Table 1 on a reference triangle T with vertices $(0, 0)$, $(1, 0)$, $(0, 1)$.

5 Miscellaneous techniques

5.1 Finite element transformation

Considering a reference triangle T with interpolation points $\{(\bar{x}_l, \bar{y}_l)\}$, given an arbitrary non-degenerate element $\mathscr{T} \in \mathcal{T}_h$ with $\{(x_l, y_l)\}$, it suffices to construct a reference finite element as triple (T, P_T, Σ_T) and an affine mapping $F_{\mathscr{T}}$, bijectively, see [5]. Then, a general finite element $(\mathscr{T}, P_{\mathscr{T}}, \Sigma_{\mathscr{T}})$ is given by

$$
\begin{aligned}
&\mathscr{T} = F_{\mathscr{T}}(T),\\
&P_{\mathscr{T}} = \{\phi_{\mathscr{T}} : \phi_{\mathscr{T}} = \phi_T \cdot F_{\mathscr{T}}^{-1}, \phi_T \in P_T\},\\
&\text{Lagrange basis} : \Sigma_{\mathscr{T}} = \{\phi_{\mathscr{T}l}(F_{\mathscr{T}}(\bar{x}_k)) = \delta_{l,k}\},\\
&\text{orthogonal basis} : \Sigma_{\mathscr{T}} = \{(\phi_{\mathscr{T}l}, \phi_{\mathscr{T}k})_{\mathscr{T}} = c_{\mathscr{T}}\delta_{l,k}, c_{\mathscr{T}} > 0\}.
\end{aligned}
$$

In constructing the discrete weak Galerkin Laplacian, derivatives of basis functions on $\mathscr{T}$ are implicitly obtained from a reference element with affine transformations. To see this, suppose that $\{\psi_l\}_{l=1}^N$ are the basis functions on the triangle element $\mathscr{T}$ and $\{\bar{\psi}_l\}_{l=1}^N$ are the corresponding basis function on the reference element T. If we write gradients $\nabla\psi_l := (\frac{\partial\psi_l}{\partial x}, \frac{\partial\psi_l}{\partial y})$, then

$$\nabla_{(\bar{x},\bar{y})}\bar{\psi}_l = \nabla(\psi_l \cdot F_{\mathscr{T}}^{-1}) = \nabla_{(x,y)}\psi_l \; B.$$

Now by using the row form of the Hessian matrix $H(\psi_l) := (\frac{\partial^2\psi_l}{\partial x^2}, \frac{\partial^2\psi_l}{\partial x\partial y}, \frac{\partial^2\psi_l}{\partial y^2})$, for the second derivative, we have

$$H(\bar{\psi}_l) = H(\psi_l \cdot F_{\mathscr{T}}^{-1}) = H(\psi_l)\Theta,$$

where Θ is a coefficient matrix. Given a reference element with vertices $(0, 0)$, $(1, 0)$, $(0, 1)$, the above formulas can be expanded in detail as

$$F_{\mathscr{T}}(\bar{\mathbf{x}}) := B\bar{\mathbf{x}} + \mathbf{b} = \begin{bmatrix} x_2 - x_1 & x_3 - x_1 \\ y_2 - y_1 & y_3 - y_1 \end{bmatrix} \begin{bmatrix} \bar{x} \\ \bar{y} \end{bmatrix} + \begin{bmatrix} x_1 \\ y_1 \end{bmatrix},$$

$$\begin{bmatrix} \frac{\partial \bar{\psi}_1}{\partial \bar{x}} & \frac{\partial \bar{\psi}_1}{\partial \bar{y}} \\ \vdots & \vdots \\ \frac{\partial \bar{\psi}_N}{\partial \bar{x}} & \frac{\partial \bar{\psi}_N}{\partial \bar{y}} \end{bmatrix} = \begin{bmatrix} \frac{\partial \psi_1}{\partial x} & \frac{\partial \psi_1}{\partial y} \\ \vdots & \vdots \\ \frac{\partial \psi_N}{\partial x} & \frac{\partial \psi_N}{\partial y} \end{bmatrix} \begin{bmatrix} x_2 - x_1 & x_3 - x_1 \\ y_2 - y_1 & y_3 - y_1 \end{bmatrix},$$

$$\begin{bmatrix} \frac{\partial^2 \bar{\psi}_1}{\partial \bar{x}^2} & \frac{\partial^2 \bar{\psi}_1}{\partial \bar{x}\partial \bar{y}} & \frac{\partial^2 \bar{\psi}_1}{\partial \bar{y}^2} \\ \vdots & \vdots & \vdots \\ \frac{\partial^2 \bar{\psi}_N}{\partial \bar{x}^2} & \frac{\partial^2 \bar{\psi}_N}{\partial \bar{x}\partial \bar{y}} & \frac{\partial^2 \bar{\psi}_N}{\partial \bar{y}^2} \end{bmatrix} = \begin{bmatrix} \frac{\partial^2 \psi_1}{\partial x^2} & \frac{\partial^2 \psi_1}{\partial x\partial y} & \frac{\partial^2 \psi_1}{\partial y^2} \\ \vdots & \vdots & \vdots \\ \frac{\partial^2 \psi_N}{\partial x^2} & \frac{\partial^2 \psi_N}{\partial x\partial y} & \frac{\partial^2 \psi_N}{\partial y^2} \end{bmatrix} \begin{bmatrix} b_{11}^2 & b_{11}b_{12} & b_{12}^2 \\ 2b_{11}b_{21} & b_{11}b_{22} + b_{21}b_{12} & 2b_{12}b_{22} \\ b_{21}^2 & b_{21}b_{22} & b_{22}^2 \end{bmatrix},$$

with $b_{11} = x_2 - x_1$, $b_{12} = x_3 - x_1$, $b_{21} = y_2 - y_1$, $b_{22} = y_3 - y_1$.

5.2 Boundary conditions

The treatment of boundary conditions in WG-FEM (see Fig. 6) is flexible compared with H^2-FEM (2.4) and mixed-FEM (2.5) methods. As pointed out, the weak function $v = \{v_0, v_b, v_g\mathbf{n}_e\} \in V_h(T)$ is represented in three parts, for which the last two parts are directly associated with the boundary conditions. If case where the Lagrange interpolation polynomial space is employed, Dirichlet boundary conditions simply require us to set $u_b(x_l) = u(x_l)$ on the corresponding interpolation points, while for Neumann boundary conditions the relation $u_g(x_l)\mathbf{n}_e \cdot \hat{n} = \nabla u(x_l) \cdot \hat{n}$ should be

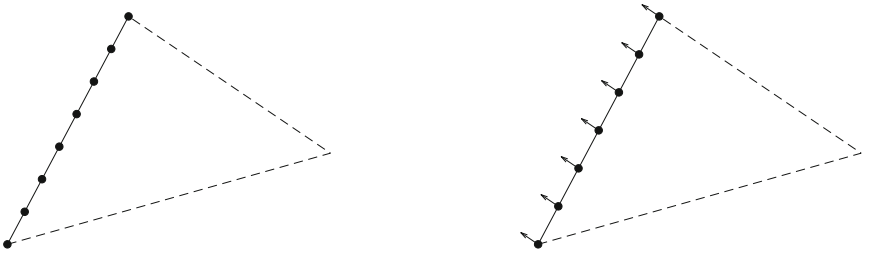

(a) $u_b : u_b(x_l) = u(x_l)$. (b) $u_g : u_g(x_l)\mathbf{n}_e \cdot \hat{n} = \nabla u(x_l) \cdot \hat{n}$.

Fig. 6 Boundary conditions for u_b, u_g

satisfied. For an orthogonal basis function space, these boundary conditions would be formulated as:

$$c_b^l < u_b^l, u_b^l >_e =< g, u_b^l >_e,\ e \in \mathcal{E}_B,$$
$$c_g^l < u_g^l \mathbf{n}_e \cdot \hat{n}, u_g^l >_e =< h, u_g^l >_e,\ e \in \mathcal{E}_B,$$

where $\{c_b^1\}$, $\{c_g^l\}$ are the corresponding boundary coefficients.

5.3 High-precision quadrature rule

A particular interest of this paper is the consideration of a potential of high convergence rates and precisions in WG-FEM. To assemble the matrix and right-hand side involves the computation of the integrals of local basis polynomials with high degree, which in turn requires the exact or approximated computation of integrals, which we will designate as $T \in \mathcal{T}_h$. Let T be a non-degenerate triangle with area $|T|$. In case where the integrand is a polynomial, it is possible to write down the integral over T exactly, using the fact that

$$\int_T x^i y^j dT = 2\,|T|\,\frac{i!j!}{(i+j+2)!}.$$

However, for general integrands, a Gauss quadrature rule can be used to estimate integrals:

$$\int_T f(x, y) dT \approx \sum_{l=1}^{Nq} w_l f(x_l, y_l),$$

where $\{x_l, y_l\}$ are quadrature points, and $\{w_l\}$ are quadrature weights. If the integrand is sufficiently smooth within T, then the accuracy of the integral approximation can be increased by using rules of increasing order. Aside from Gaussian quadrature rules, there are other rules such as those of Dunavant [7] or Lyness [13], whose tabulated values of quadrature points and weights can be used.

6 Numerical experiments

We present several studies to demonstrate the high accuracy and robustness of Algorithm 1. Note that the Lesbegue measures of degenerated $(d-1)$-dimensional space, i.e., the edges and boundaries, are zeros; we only consider errors over the interior of elements. The errors will be measured in three norms

$$\|u\|_{L^2}^2 = \sum_{T\in\mathcal{T}_h} \int_T |u_0|^2\, dx,$$
$$\|u\|_{H^1}^2 = \sum_{T\in\mathcal{T}_h} \int_T |\nabla u_0|^2 + |u_0|^2\, dx,$$
$$\|u\|_{H^2}^2 = \sum_{T\in\mathcal{T}_h} \int_T |\Delta u_0|^2 + |\nabla u_0|^2 + |u_0|^2\, dx.$$

6.1 Case 1

Consider the biharmonic problem seeking a function $u = u(x, y)$ that satisfies

$$\Delta^2 u = f,$$

in an unit square $\Omega = [0, 1]^2$, with boundary conditions and right-hand side function $f(x, y)$ chosen so that the exact solution is $u(x, y) = (x - y)^{20}/380$. Uniform triangulations $\{\mathcal{T}_h\}$ are used and the estimated convergence rates are defined by

$$\log(\|u - u_{h/2}\|)/\log(\|u - u_h\|),$$

where u_h is the numerical solution on the mesh $\mathcal{T}_h$. The uniform triangulation $\mathcal{T}_h$ was constructed as follows: partition the unit square domain into $n \times n$ uniform subrectangles, then split each square element along the diagonal. The mesh size of $\mathcal{T}_h$ is denoted by $h = 1/n$. Table 2 shows the convergence errors and convergence rates for WG-FEM with weak function spaces from P_3 to P_{10}. In this and subsequent tests, we use $\alpha_T = (\max |e|)^{-3}$ and $\beta_T = (\max \|e\|)^{-1}$, $e \in \partial T$ on the element $T \in \mathcal{T}_h$. The basis functions are constructed by starting with Lagrange interpolation polynomial space defined on Gauss-Lobatto points, which are then orthogonalized with the Levenberg-Marquardt method discussed above. Meanwhile, the numerical tests show that, in most cases, the hierarchical basis by itself cannot provide computational results of desired accuracy. However, it can be used to construct other kinds of basis functions. The discrete weak function space is defined as follows

$$\begin{aligned} V_h(\Omega) &= \{v = \{v_0, v_b, v_g \mathbf{n}_e\} : v|_T \in V_h(T), T \in \mathcal{T}_h\}, \\ V_h(T) &= \{v_0 \in P_l(T), v_b \in P_l(e), v_g \in P_{l-1}(e), e \subset \partial T\}. \end{aligned}$$

We lower the maximum degree by 2 for the discrete weak Laplacian space

$$G_h(\Omega) = \{v_w : v_w \in P_{l-2}(T), T \in \mathcal{T}_h\}.$$

The tests used double-precision arithmetic. The tables below correspond to the $l = 3$ to $l = 10$, successively. Table 2 shows that the WG-FEM convergence rates are the same as for classical FEM. In the last table, the anomalies in the final line arise simply because the method has converged to the tolerance and little more progress can be made.

6.2 Case 2

As we have already pointed out, the polynomial space for the weak function and weak Laplacian function can be selected from different kinds of polynomial spaces. In this test, we intend to study the influence of the weak Laplacian space to the WG-FEM, and see what is the best choice for the weak Laplacian space $G_h(\Omega)$ given a weak function polynomial space $V_h(\Omega)$. Here, we employ a supported plate problem, see [2], with an exact solution

$$u(x, y) = \alpha \sin(m\pi x) \sin(n\pi y),$$

on an unit square domain. We choose $m = n = 4$, and $\alpha = 1/16\pi^2$. We use the same meshes as in Case 1. The right hand of this problem is highly oscillatory, but

Table 2 Errors and convergence rates with orthogonal basis from P_3 to P_{10}

$l=3,\ \Delta h$	$\|\|u-u_h\|\|_{L^2}$	Rate	$\|\|u-u_h\|\|_{H^1}$	Rate	$\|\|u-u_h\|\|_{H^2}$	Rate
1/4	5.954E−02	–	5.570E−01	–	1.088E+01	–
1/8	5.176E−03	3.524	5.573E−02	3.321	2.057E+00	2.404
1/16	3.939E−04	3.716	8.784E−03	2.666	6.267E−01	1.715
1/32	2.666E−05	3.885	1.437E−03	2.611	1.933E−01	1.697
$l=4,\ \Delta h$	$\|\|u-u_h\|\|_{L^2}$	Rate	$\|\|u-u_h\|\|_{H^1}$	Rate	$\|\|u-u_h\|\|_{H^2}$	Rate
1/4	4.687E−02	–	1.035E+00	–	2.471E+01	–
1/8	1.881E−03	4.639	8.079E−02	3.679	3.805E+00	2.699
1/16	5.906E−05	4.993	4.973E−03	4.022	4.738E−01	3.006
1/32	1.840E−06	5.004	3.067E−04	4.019	5.976E−02	2.987
$l=5,\ \Delta h$	$\|\|u-u_h\|\|_{L^2}$	Rate	$\|\|u-u_h\|\|_{H^1}$	Rate	$\|\|u-u_h\|\|_{H^2}$	Rate
1/4	1.878E−02	–	7.078E−01	–	2.900E+01	–
1/8	3.824E−04	5.618	2.872E−02	4.623	2.358E+00	3.620
1/16	6.205E−06	5.946	9.330E−04	4.944	1.550E−01	3.928
1/32	9.990E−08	5.957	3.003E−05	4.957	1.003E−02	3.949
$l=6,\ \Delta h$	$\|\|u-u_h\|\|_{L^2}$	Rate	$\|\|u-u_h\|\|_{H^1}$	Rate	$\|\|u-u_h\|\|_{H^2}$	Rate
1/4	6.028E−03	–	3.317E−01	–	2.047E+01	–
1/8	5.918E−05	6.670	6.524E−03	5.668	8.089E−01	4.661
1/16	4.748E−07	6.962	1.045E−04	5.964	2.610E−02	4.954
1/32	3.791E−09	6.969	1.666E−06	5.972	8.365E−04	4.963
$l=7,\ \Delta h$	$\|\|u-u_h\|\|_{L^2}$	Rate	$\|\|u-u_h\|\|_{H^1}$	Rate	$\|\|u-u_h\|\|_{H^2}$	Rate
1/4	1.390E−03	–	1.021E−01	–	8.752E+00	–
1/8	6.630E−06	7.712	9.751E−04	6.710	1.677E−01	5.706
1/16	2.682E−08	7.950	7.855E−06	6.956	2.702E−03	5.956
1/32	1.080E−10	7.956	6.292E−08	6.964	4.318E−05	5.967
$l=8,\ \Delta h$	$\|\|u-u_h\|\|_{L^2}$	Rate	$\|\|u-u_h\|\|_{H^1}$	Rate	$\|\|u-u_h\|\|_{H^2}$	Rate
1/4	2.503E−04	–	2.299E−02	–	2.575E+00	–
1/8	5.739E−07	8.769	1.055E−04	7.768	2.365E−02	6.766
1/16	1.159E−09	8.951	4.238E−07	7.959	1.899E−04	6.961
1/32	2.343E−12	8.951	1.705E−09	7.958	1.526E−06	6.959
$l=9,\ \Delta h$	$\|\|u-u_h\|\|_{L^2}$	Rate	$\|\|u-u_h\|\|_{H^1}$	Rate	$\|\|u-u_h\|\|_{H^2}$	Rate
1/4	3.506E−05	–	3.874E−03	–	5.440E−01	–
1/8	3.883E−08	9.818	8.567E−06	8.821	2.405E−03	7.821
1/16	3.921E−11	9.952	1.718E−08	8.962	9.608E−06	7.968
1/32	4.311E−14	9.829	3.589E−11	8.903	3.991E−08	7.911
$l=10,\ \Delta h$	$\|\|u-u_h\|\|_{L^2}$	Rate	$\|\|u-u_h\|\|_{H^1}$	Rate	$\|\|u-u_h\|\|_{H^2}$	Rate
1/4	3.883E−06	–	5.000E−04	–	8.526E−02	–
1/8	2.074E−09	10.870	5.325E−07	9.875	1.813E−04	8.877
1/16	1.050E−12	10.948	5.342E−10	9.961	3.620E−07	8.968
1/32	6.214E−14	4.079	3.051E−11	4.130	3.403E−08	3.411

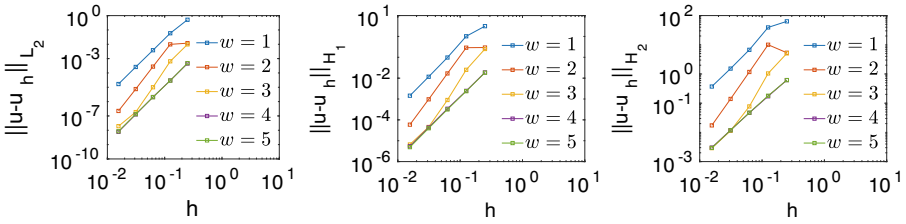

Fig. 7 Weak function space $l = 3$, weak Laplacian space $w = 1, \cdots, 5$

the weak Galerkin method can efficiently deal with this phenomenon. The discrete weak function space is defined as

$$V_h(\Omega) = \{v = \{v_0, v_b, v_g \mathbf{n}_e\} : v|_T \in V_h(T), T \in \mathcal{T}_h\},$$
$$V_h(T) = \{v_0 \in P_l(T), v_b \in P_l(e), v_g \in P_{l-1}(e), e \subset \partial T\}.$$

For the given weak function space, we consider a sequence of different discrete weak Laplacian spaces

$$G_h(\Omega) = \{v_w : v_w|_T \in P_w(T), T \in \mathcal{T}_h\}, w = l-2, \ldots, l+2.$$

The slope of the lines in Figs. 7, 8, 9 indicates the convergence orders, showing L^2 convergence rates of 4, 5, 6, H^1 rates of 3, 4, 5, and H^2 rates of 2, 3, 4, respectively. Figures 7, 8, and 9 show that the convergence rate depends primarily on the interior basis space, not the weak Laplacian space. However, for a given interior space, increasing the degree of the weak Laplacian space does make the L^2, H^1, H^2 convergence errors decrease faster. The results suggest that, for a given interior space, the best choice for the weak Laplacian space may be one degree higher than the interior space.

6.3 Case 3

In this case, we employ the examples from Case 1 and Case 2 to investigate some other issues. Let us check how different basis functions influence the discrete system and the sparsity of the global matrix with orthogonal basis. Based on Case 1, the

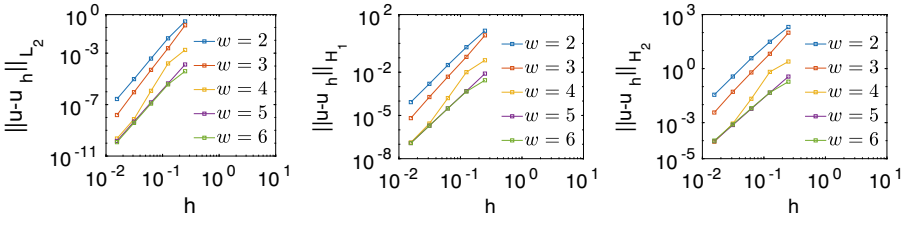

Fig. 8 Weak function space $l = 4$, weak Laplacian space $w = 2, \cdots, 6$

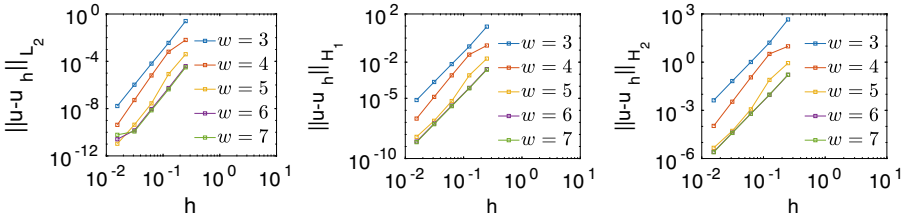

Fig. 9 Weak function space $l = 5$, weak Laplacian space $w = 3, \cdots, 7$

discrete weak function space is defined as

$$V_h(\Omega) = \{v = \{v_0, v_b, v_g \mathbf{n}_e\} : v|_T \in V_h(T), T \in \mathcal{T}_h\},$$
$$V_h(T) = \{v_0 \in P_l(T), v_b \in P_l(e), v_g \in P_{l-1}(e), e \subset \partial T\}.$$

where $l = 7, 8, 9, 10$, respectively, and the discrete weak Laplacian space is

$$G_h(\Omega) = \{v_w : v_w|_T \in P_{l-2}(T), T \in \mathcal{T}_h\}.$$

We consider the basis functions of Lagrange interpolation polynomials on the Gaussian Lobatto quadrature points and their corresponding orthogonal polynomial basis functions constructed by applying the Levenberg-Marquardt method (identified in the plots by the prefix LM). Figure 10a compares convergence errors for the Lagrange

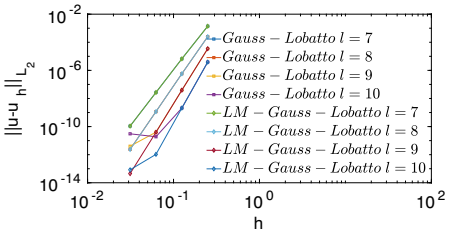

(a) Gauss Lobatto.

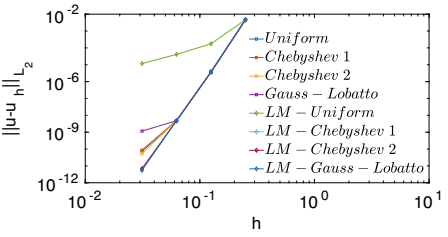

(b) Different basis.

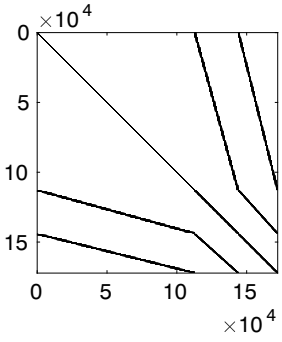

(c) Global sparse matrix.

Fig. 10 Numerical results for Case 3

and orthogonal basis functions. The discrete weak Galerkin space for Fig. 10b and c is defined as:

$$V_h(\Omega) = \{v = \{v_0, v_b, v_g \mathbf{n}_e\} : v|_T \in V_h(T), T \in \mathcal{T}_h\},$$
$$V_h(T) = \{v_0 \in P_9(T), v_b \in P_9(e), v_g \in P_8(e), e \subset \partial T\}.$$

and the discrete weak Laplacian space as

$$G_h(\Omega) = \{v_w : v_w|_T \in P_7(T), T \in \mathcal{T}_h\}.$$

Considering Case 2 again, Fig. 10a and b show the computational results with different basis functions. It may be observed that, with decreasing mesh size and increasing basis function degree, computational results with the Lagrange basis lose precision, whereas the results for the orthogonal basis are not so affected. While orthogonalization by itself seems most helpful, better results have been observed when the orthogonalization processes are applied to Lagrange basis functions associated with Gauss-Lobatto points rather than uniformly spaced points. Figure 10c displays the structure of the global sparse matrix generated using the orthogonal LM-Gauss-Lobatto basis function with mesh size $h = 1/32$. The number of unknowns for this problem is 172,224, and the system matrix has 24,334,272 nonzero entries, which implies a highly sparse system of density 8.2E−4.

7 Conclusions

WG-FEM represents a new variation of the classic finite element method. The concept of weakness is applied across the board, so that we must consider weak functions, weak gradients, and weak Laplacian operators. The method is very flexible in dealing with boundary conditions, whether of Dirichlet or Neumann type. It is a powerful tool for studying fourth-order problem. The method can be extended to an adaptive hp-WG-FEM method. It is hoped that this paper has provided a helpful perspective encouraging the investigation and use of WG-FEM for high-precision simulations.

Funding information John Burkardt was supported in part by the US Air Force Office of Scientific Research grant FA9550-15-1-0001. Max Gunzburger was supported in part by the US Air Force Office of Scientific Research grant FA9550-15-1-0001. Wenju Zhao was supported in part by the US Air Force Office of Scientific Research grant FA9550-15-1-0001.

Compliance with Ethical Standards

Conflict of interest The authors declare that they have no conflict of interest.

References

1. Adams, R.A., Fournier, J.J.F.: Sobolev Spaces. Pure and Applied Mathematics (Amsterdam), 2nd edn., vol. 140. Elsevier/Academic Press, Amsterdam (2003)

2. Arad, M., Yakhot, A., Ben-Dor, G.: A highly accurate numerical solution of a biharmonic equation. Numer. Methods Partial Differential Equations **13**(4), 375–391 (1997)
3. Berrut, J.-P., Trefethen, L.N.: Barycentric Lagrange interpolation. SIAM Rev. **46**(3), 501–517 (electronic) (2004)
4. Burkardt, J.: The finite element basis for simplices in arbitrary dimensions (2011)
5. Ciarlet, P.G.: The Finite Element Method for Elliptic Problems. Classics in Applied Mathematics, vol. 40, pp. xxviii+530. Society for Industrial and Applied Mathematics (SIAM), Philadelphia. Reprint of the 1978 original [North-Holland, Amsterdam; MR0520174 (58 #25001)] (2002)
6. Domínguez, V., Sayas, F.-J.: Algorithm 884: a simple Matlab implementation of the Argyris element. ACM Trans. Math. Softw. **35**(2), Art. 16, 11 (2009)
7. Dunavant, D.A.: High degree efficient symmetrical Gaussian quadrature rules for the triangle. Int. J. Numer. Methods Eng. **21**(6), 1129–1148 (1985)
8. Durán, A.J., Van Assche, W.: Orthogonal matrix polynomials and higher-order recurrence relations. Linear Algebra Appl. **219**, 261–280 (1995)
9. Farouki, R.T., Goodman, T.N.T., Sauer, T.: Construction of orthogonal bases for polynomials in Bernstein form on triangular and simplex domains. Comput. Aided Geom. Des. **20**(4), 209–230 (2003)
10. Gautschi, W.: Orthogonal Polynomials: Computation and Approximation. Numerical Mathematics and Scientific Computation. Oxford University Press, New York (2004). Oxford Science Publications
11. Guan, Q., Gunzburger, M., Zhao, W.: Weak-Galerkin finite element methods for a second-order elliptic variational inequality. Comput. Methods Appl. Mech. Eng. **337**, 677–688 (2018)
12. Hesthaven, J.S.: From electrostatics to almost optimal nodal sets for polynomial interpolation in a simplex. SIAM J. Numer. Anal. **35**(2), 655–676 (1998)
13. Lyness, J.N., Jespersen, D.: Moderate degree symmetric quadrature rules for the triangle. J. Inst. Math. Appl. **15**, 19–32 (1975)
14. Monk, P.: A mixed finite element method for the biharmonic equation. SIAM J. Numer. Anal. **24**(4), 737–749 (1987)
15. Moré, J.J.: The Levenberg-Marquardt algorithm: implementation and theory. In: Watson, G.A. (ed.) Numerical Analysis: Proceedings of the Biennial Conference Held at Dundee, June 28–July 1, 1977, pp. 105–116. Springer, Berlin (1978)
16. Mozolevski, I., Süli, E.: A priori error analysis for the *hp*-version of the discontinuous Galerkin finite element method for the biharmonic equation. Comput. Methods Appl. Math. **3**(4), 596–607 (2003)
17. Mu, L., Wang, J., Wang, Y., Ye, X.: A weak Galerkin mixed finite element method for biharmonic equations. In: Numerical Solution of Partial Differential Equations: Theory, Algorithms, and their Applications. Springer Proc. Math. Stat., vol. 45, pp. 247–277. Springer, New York (2013)
18. Mu, L., Wang, J., Wang, Y., Ye, X.: A computational study of the weak Galerkin method for second-order elliptic equations. Numer. Algorithms **63**(4), 753–777 (2013)
19. Mu, L., Wang, J., Ye, X.: Weak Galerkin finite element methods for the biharmonic equation on polytopal meshes. Numer. Methods Partial Differential Equations **30**(3), 1003–1029 (2014)
20. Wang, C., Wang, J.: An efficient numerical scheme for the biharmonic equation by weak Galerkin finite element methods on polygonal or polyhedral meshes. Comput. Math. Appl. **68**(12, part B), 2314–2330 (2014)
21. Wang, C., Wang, J.: A hybridized weak Galerkin finite element method for the biharmonic equation. Int. J. Numer. Anal. Model. **12**(2), 302–317 (2015)
22. Wang, J., Ye, X.: A weak Galerkin finite element method for second-order elliptic problems. J. Comput. Appl. Math. **241**, 103–115 (2013)
23. Wang, C., Wang, J.: Weak Galerkin finite element methods for elliptic PDEs. Scientia Sinica Mathematica **45**(7), 1061–1092 (2015)
24. Zhang, S.: On the full C_1-Q_k finite element spaces on rectangles and cuboids. Adv. Appl. Math. Mech. **2**(6), 701–721 (2010)